Chapter 37

High Content Screening Biosensor Assay to Identify Disruptors of p53–hDM2 Protein-Protein Interactions

Yun Hua, Christopher J. Strock, and Paul A. Johnston

Abstract

This chapter describes the implementation of the p53–hDM2 protein-protein interaction (PPI) biosensor (PPIB) HCS assay to identify disruptors of p53–hDM2 PPIs. Recombinant adenovirus expression constructs were generated bearing the individual p53–GFP and hDM2–RFP PPI partners. The N-terminal p53 transactivating domain that contains the binding site for hDM2 is expressed as a GFP fusion protein that is targeted and anchored in the nucleolus of infected cells by a nuclear localization (NLS) sequence. The p53–GFP biosensor is localized to the nucleolus to enhance and facilitate the image acquisition and analysis of the PPIs. The N-terminus of hDM2 encodes the domain for binding to the transactivating domain of p53, and is expressed as a RFP fusion protein that includes both an NLS and a nuclear export sequence (NES). In U-2 OS cells co-infected with both adenovirus constructs, the binding interactions between hDM2 and p53 result in both biosensors becoming co-localized within the nucleolus. Upon disruption of the p53–hDM2 PPIs, the p53–GFP biosensor remains in the nucleolus while the shuttling hDM2–RFP biosensor redistributes into the cytoplasm. p53–hDM2 PPIs are measured by acquiring fluorescent images of cells co-infected with both adenovirus biosensors on an automated HCS imaging platform and using an image analysis algorithm to quantify the relative distribution of the hDM2–RFP shuttling component of the biosensor between the cytoplasm and nuclear regions of compound treated cells.

Key words Protein-protein interaction biosensors, High content screening, Imaging, Image analysis

1 Introduction

The combination of high content screening (HCS) with fluorescent biosensors allows for high spatial and temporal resolution of protein-protein interaction (PPI) partners that have been fused to spectrally distinct fluorescent reporter proteins [1–9]. The distribution of macromolecules within compartments of the cell is a tightly regulated process, exemplified by the passage of proteins through the nuclear pore complexes (NPCs) in the nuclear envelope that separates the cytoplasm and nucleus [10]. While small molecules pass through NPCs by passive diffusion, the passage of cargos larger than ~40 kDa require a facilitated active import and

Cheryl L. Meyerkord and Haian Fu (eds.), *Protein-Protein Interactions: Methods and Applications*, Methods in Molecular Biology, vol. 1278, DOI 10.1007/978-1-4939-2425-7_37,

export process mediated by specific receptor proteins [10]. Passage through the NPC involves the assembly of a trimeric import-complex in the cytoplasm between an importin-α adaptor receptor that recognizes the nuclear localization sequence (NLS) of the cargo and the importin-β transport receptor that facilitates docking interactions with the nucleoporins [10, 11]. Since the nucleus and cytoplasm represent subcellular compartments that can readily be distinguished by HCS methods, investigators have taken advantage of the regulated nucleocytoplasmic transport of proteins to design biosensors to measure PPIs [1, 2, 4, 5]. To construct translocation or positional biosensors, the "bait" biosensor is typically anchored to a specific location within the cell while the "prey" biosensor is designed to shuttle between different compartments or regions of the cell, and productive PPIs are required for the co-localization of both biosensors [1, 2, 4, 5].

In an example involving p53 and hDM2, Stauber and colleagues generated a "bait" biosensor encoding the interacting domain of p53 fused to HIV-1 Rev and blue fluorescent protein (BFP) that when transfected into cells was expressed in the nucleolus region of the nucleus [5]. They constructed a shuttling "prey" biosensor encoding the interacting domain of mdm2 fused with a SV40 NLS sequence, an HIV-1 Rev NES sequence, GST, and green fluorescent protein (GFP) to generate an NLS-GFP-GST-mdm2-NES expression plasmid that when transfected into cells was predominantly localized in the cytoplasm [5]. Co-transfection of cells with both the p53 "bait" and mdm2 "prey" biosensors resulted in translocation of the mdm2 biosensor into the nucleus and co-localization with the p53 biosensor in the nucleolus [5]. Nutlin-3 treatment of cells co-transfected with both biosensors caused a redistribution of the mdm2 prey biosensor into the cytoplasm [5]. We have recently described the development and implementation of a similarly designed p53–hDM2 protein-protein interaction biosensor (PPIB) HCS assay in which we screened 220,017 of the NIH's compound library and identified three novel structurally related methylbenzo-naphthyridin-5-amine (MBNA) hits [1, 2]. Hit follow-up studies revealed that the MBNAs triggered the expected biological responses, including enhanced p53 protein and p53 target gene levels, p53-dependent cell cycle arrest in G1, apoptosis, and growth inhibition with IC_{50}s ~4 μM [2].

This chapter describes the employment of the p53–hDM2 PPIB HCS assay to identify p53–hDM2 PPI disruptors [1, 2]. Recombinant adenovirus expression constructs were created for the individual p53–GFP and hDM2–RFP PPI partners (Fig. 1). The N-terminal residues 1–131 of p53 include the p53 transactivating domain that contains the binding site for hDM2. This GFP fusion protein fragment is targeted to and anchored in the nucleolus by the inclusion of nuclear localization (NLS) and nucleolus

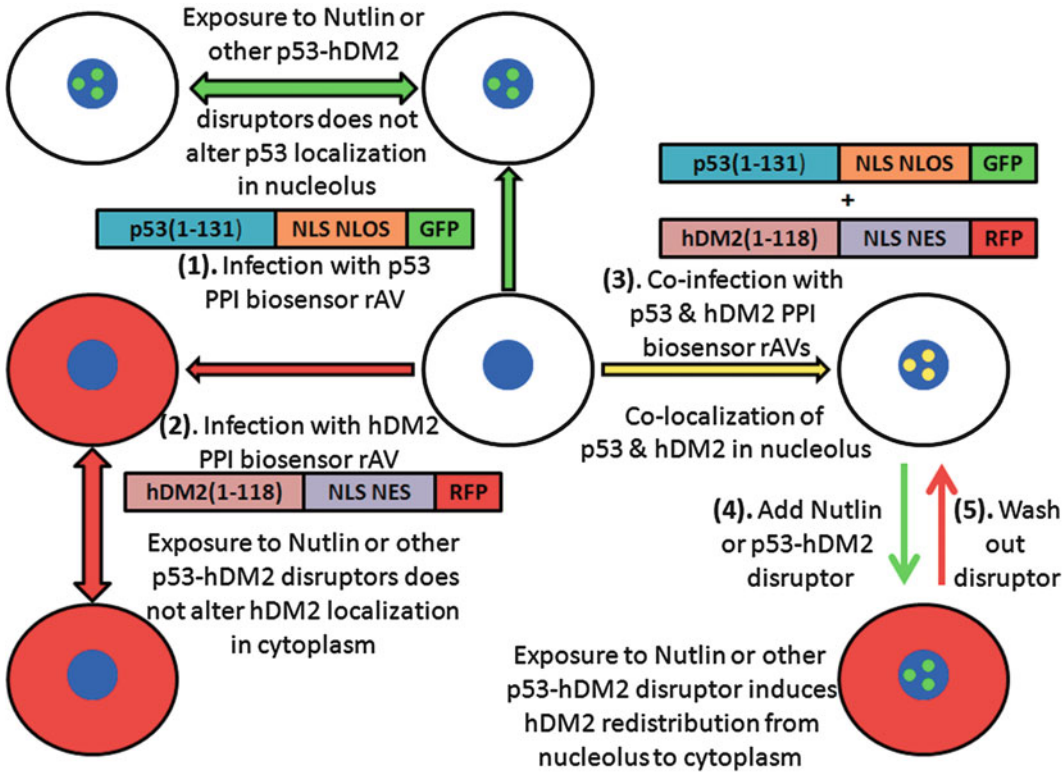

Fig. 1 p53–hDM2 protein-protein interaction biosensor design and distribution phenotypes. Recombinant adenovirus expression constructs were generated bearing the individual p53–GFP and hDM2–RFP PPI partners. The N-terminal residues 1–131 of p53 include the transactivating domain that contains the binding site for hDM2, and this protein fragment is expressed as a GFP fusion protein that is targeted and anchored in the nucleolus of infected cells by the inclusion of nuclear localization (NLS) and nucleolus localization (NLOS) sequences. The p53–GFP component is directed to the nucleolus to enhance and facilitate the image acquisition and analysis of the PPIs. *Route 1*: In cells infected with the p53–GFP "bait" biosensor adenovirus alone, the p53–GFP remains localized to bright fluorescent puncta in the nucleolus and its distribution does not alter upon exposure to Nutlin-3 or other p53–hDM2 disruptors. The N-terminal residues 1–118 of hDM2 encode the domain for binding to the p53 transactivating domain, and this fragment is expressed as a RFP fusion protein that includes both an NLS and a nuclear export sequence (NES). *Route 2*: In cells infected with the hDM2–RFP adenovirus "prey" biosensor alone, hDM2–RFP expression is localized only in the cytoplasm of cells and does not change upon exposure to Nutlin-3 or other p53–hDM2 disruptors. *Route 3*: In U-2 OS cells that are co-infected with both adenovirus constructs, however, the binding interactions between the hDM2 and p53 components of the biosensors result in both proteins becoming localized to the nucleolus. *Route 4*: Upon disruption of the p53–hDM2 protein-protein interaction with a compound like Nutlin-3, the p53–GFP interaction partner remains nucleolar, while the shuttling hDM2–RFP interaction partner redistributes into the cytoplasm. *Route 5*: Upon removal of a disrupting agent like Nutlin 3, the shuttling hDM2–RFP interaction partner redistributes back into the p53–GFP containing nucleolus

localization (NLOS) sequences (Fig. 1) [1, 2], which enhances and facilitates image acquisition and analysis of the PPIs. In cells infected with the p53–GFP "bait" biosensor adenovirus alone, the p53–GFP remains localized to bright fluorescent puncta in

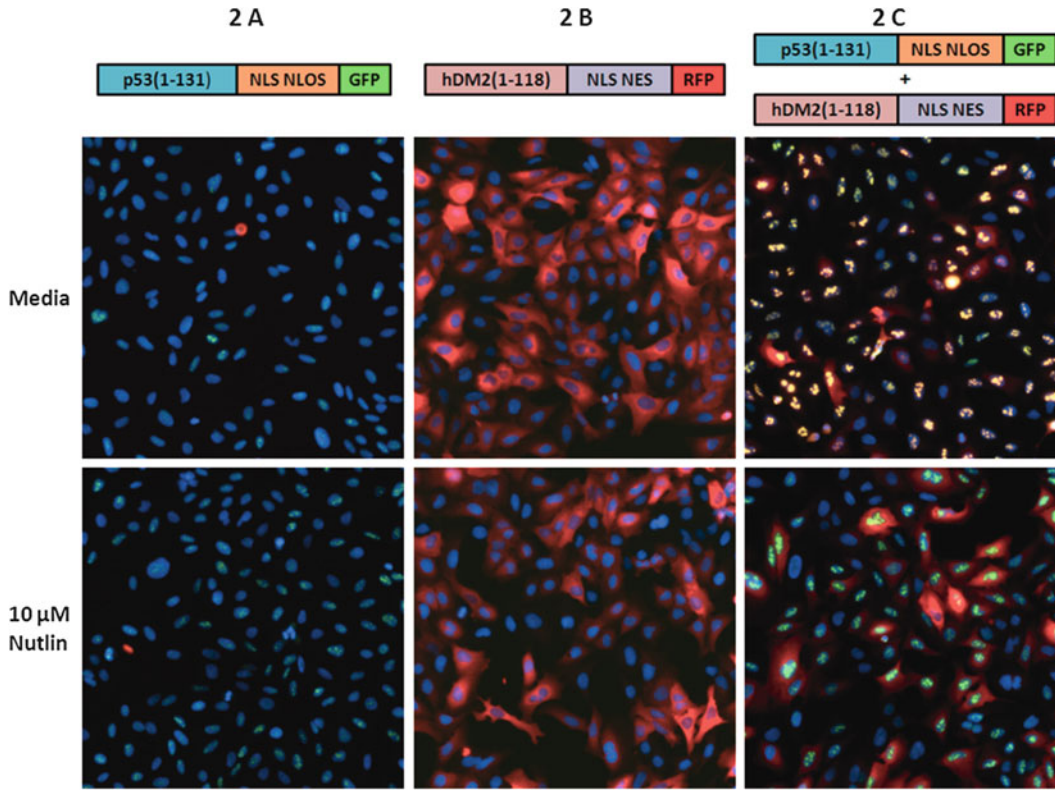

Fig. 2 Color composite images of U-2 OS cells infected with (**a**) the p53–GFP biosensor alone, (**b**) the hDM2–RFP biosensor alone, or (**c**) co-infected with both biosensors and then treated ± 10 μM Nutlin-3 for 90 min. U-2 OS cells were infected with (**a**) the p53–GFP biosensor alone, (**b**) the hDM2 biosensor alone, or (**c**) co-infected with both biosensors and 2,500 cells were seeded into the wells of 384-well assay plates, cultured overnight at 37 °C, 5 % CO_2, and 95 % humidity, and then treated ± 10 μM Nutlin-3 for 90 min. Cells were then fixed and stained with Hoechst 33342 and 20× 0.4 NA images of three fluorescent channels (Ch1—Hoechst *blue*, Ch2—p53–GFP *green*, and Ch3—hDM2–RFP *red*) were acquired on the ArrayScan V^{TI} automated imaging platform as described above. Representative color composite images of control and Nutlin-3 treated U-2 OS cells individually infected with or co-infected with both the p53–GFP and hDM2–RFP biosensors are presented. In cells infected with each of the biosensors alone, the p53–GFP biosensor remains localized to bright fluorescent puncta within the nucleoli of Hoechst stained nuclei and its distribution does not alter upon exposure to Nutlin-3, while the hDM2–RFP biosensor remains localized in the cytoplasm of cells and does not change upon exposure to Nutlin-3. In U-2 OS cells co-infected with both biosensors, however, the two biosensors become co-localized to the nucleolus, and upon exposure to Nutlin-3 the hDM2–RFP interaction partner redistributes into the cytoplasm while the p53–GFP interaction partner remains nucleolar

the nucleolus and its distribution does not alter upon exposure to Nutlin-3 or when co-infected with the hDM2–RFP biosensor (Figs. 1, route 1 and 2a). The N-terminal residues 1–118 of hDM2 encode the domain for binding to the N-terminal transactivating domain of p53, and this fragment is expressed as a RFP fusion protein that includes both an NLS and a nuclear export sequence (NES) (Fig. 1) [1, 2]. In cells infected with the hDM2–RFP adenovirus "prey" biosensor alone, hDM2–RFP

expression is localized only in the cytoplasm of cells and does not change upon exposure to Nutlin-3 (Figs. 1, route 2 and 2b). In cells that are co-infected with both adenovirus constructs, however, the interaction of the hDM2 and p53 components of the biosensors results in both proteins becoming localized to the nucleolus (Figs. 1, route 3 and 2c) [1, 2]. Upon disruption of the p53–hDM2 protein-protein interaction with a compound like Nutlin-3, the p53–GFP interaction partner remains nucleolar, while the shuttling hDM2–RFP interaction partner redistributes into the cytoplasm (Figs. 1, route 4 and 2c) [1, 2].

The disruption of the p53–HDM2 interaction biosensor is measured by acquiring images on an automated HCS imaging platform, and an image analysis algorithm is used to quantify the relative distribution of the hDM2–RFP shuttling component of the biosensor between the cytoplasm and nuclear regions of compound treated cells that were co-infected with both adenovirus biosensors (Figs. 2 and 3) [1, 2]. The images of the three fluorescent channels (Hoechst, GFP, and RFP) of the p52–hDM2 PPIB were analyzed using the molecular translocation image analysis algorithm (Fig. 3a). The nucleic acid dye Hoechst 33342 was used to stain and identify the nucleus, and this fluorescent signal was used to focus the instrument and define a nuclear mask in channel 1 (Ch1). Objects in Ch1 that exhibited the appropriate fluorescent intensities above background and size (width, length, and area) characteristics were identified and classified by the image segmentation as nuclei (dark blue ring, Ch1). The nuclear mask was eroded 1 pixel to reduce cytoplasmic contamination within the nuclear area, and the reduced mask was used to quantify the amount of target channel, p53–GFP (Ch2) or hDM2–RFP (Ch3), fluorescence within the nucleus (yellow Circ masks in Ch2 and Ch3). The nuclear mask was then dilated to cover as much of the cytoplasmic region as possible without going outside the cell boundary. Removal of the original nuclear region from this dilated mask creates a Ring mask that covers the cytoplasmic region outside the nuclear envelope (magenta Ring mask in Ch2 and cyan Ring mask in Ch3). The image analysis algorithm outputs quantitative data such as: the total and average fluorescent intensities of the Hoechst stained objects (Ch1) the selected object or cell count from Ch1, the total and average fluorescent intensities of the p53–GFP (Ch2) and the hDM2–RFP (Ch3) signals in the nucleus (Circ) or cytoplasm (Ring) regions as an overall well average value, or on an individual cell basis. To quantify the translocation of the hDM2–RFP from the nucleus to the cytoplasm induced by disruptors of the p53–hDM2 protein-protein interaction the image analysis algorithm calculates a mean average intensity difference by subtracting the average hDM2–RFP intensity in the Ring (Cytoplasm) region from the average hDM2–RFP intensity in the Circ (Nuclear) region of Ch3; Mean Circ-Ring Average Intensity Difference Channel 3

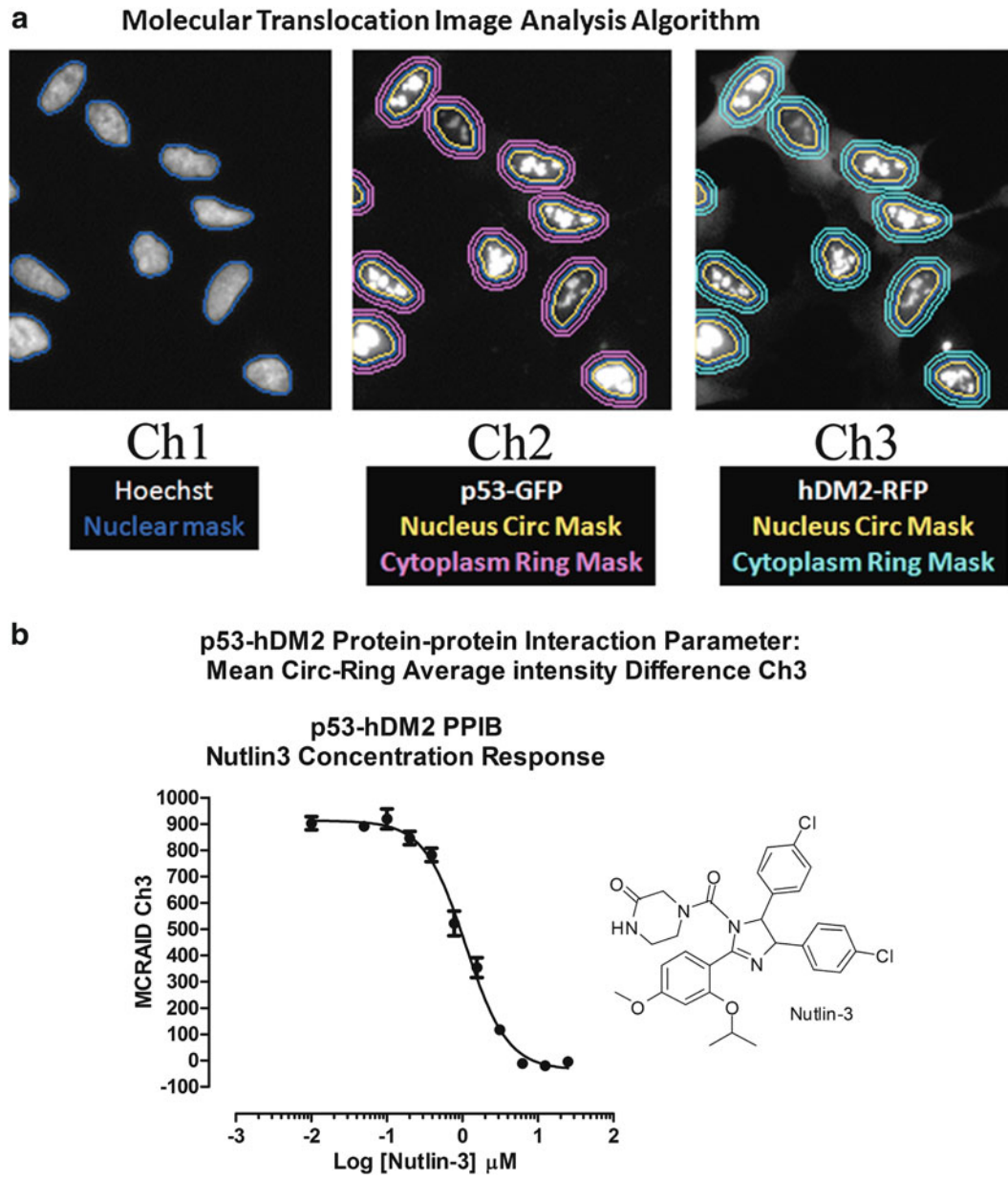

Fig. 3 Molecular translocation image analysis algorithm. U-2 OS cells co-infected with the p53–hDM2 PPIB adenoviruses were seeded at 2,500 cells per well in 384-well Greiner collagen-coated assay plates, cultured overnight at 37 °C, 5 % CO_2, and 95 % humidity, and were then exposed to the indicated concentrations of Nutlin-3 in 0.5 % DMSO for 90 min prior to fixation with 3.7 % formaldehyde containing 2 μg/mL Hoechst 33342. Images in three fluorescent channels were sequentially acquired on the ArrayScan VTI platform using a 20× 0.4 NA objective with the XF93 excitation and emission filter set and were analyzed with the molecular translocation (MT) image analysis algorithm. (**a**) Image segmentation. In Ch1, Hoechst stained objects that exhibited the appropriate morphological characteristics (width, length, and area) with fluorescent intensities sufficiently above a background threshold were identified and classified by the image segmentation as nuclei. The nuclear mask derived from Ch1 (*dark blue ring*) was then used to segment the images from Ch2 and Ch3

(MCRAID-Ch3) (Fig. 3b). On average, Nutlin-3 exhibited an IC_{50} of 0.608 ± 0.382 μM ($n = 5$) in the p53–hDM2 PPIB assay (Fig. 3b). To implement the p53–hDM2 PPIB assay in screening, the mean MCRAID-Ch3 value of the DMSO maximum plate control wells ($n = 32$) and the mean MCRAID-Ch3 value of the 10 μM Nutlin-3 minimum plate control wells ($n = 24$) were utilized to normalize the MCRAID-Ch3 compound data and to represent 0 % and 100 % disruption/inhibition of the p53–hDM2 interactions, respectively [1, 2].

2 Materials

1. Nutlin-3.
2. Formaldehyde.
3. Dimethyl sulfoxide (DMSO) (99.9 % high performance liquid chromatography-grade, under argon).
4. Hoechst 33342.
5. U-2 OS osteosarcoma cell line.
6. Culture medium: McCoy's 5A medium, 2 mM L-glutamine, 10 % fetal bovine serum, and 100 U/mL penicillin and streptomycin.
7. Humidified incubator at 37 °C, 5 % CO_2, and 95 % humidity.
8. Dulbecco's Mg^{2+} and Ca^{2+} free phosphate buffered saline (PBS).

Fig. 3 (continued) into nuclear (*Circ*) and cytoplasmic (*Ring*) regions. To reduce cytoplasm contamination within the nuclear area the nuclear mask was eroded, and the reduced mask (*yellow ring*) was used to quantify the amount of target channel, p53–GFP in Ch2 and hDM2–RFP in Ch3, fluorescence within the nuclear region. To measure fluorescence in a region of the cytoplasm in Ch2 and Ch3, the nuclear mask derived from Ch1 was dilated to cover as much of the cytoplasm region as possible without going outside the cell boundary. Removal of the original nuclear region from this dilated mask creates a ring mask that covers the cytoplasm region outside the nuclear envelope. The number of pixels away from the nuclear mask and the number of pixels (width) between the inner and outer ring masks were selectable within the MT bio-application software. The ring masks were then used to quantify the amount of target channel, p53–GFP (Ch2, *mauve rings*) or hDM2–RFP (Ch3, *light blue rings*), fluorescence within the cytoplasm region. (**b**) Chemical structure of Nutlin-3 and concentration dependent disruption of p53–hDM2 PPIs. The molecular translocation image analysis algorithm produces a mean average intensity difference in Ch3 (MCRAID-Ch3) parameter calculated by subtracting the average hDM2–RFP intensity in the *Ring* (Cytoplasm) region from the average hDM2–RFP intensity in the *Circ* (Nuclear) region of Ch3. High MCRAID-Ch3 values indicate that the hDM2–RFP biosensor is predominantly localized within the nuclear region, while low MCRAID-Ch3 values indicate a more prominent localization within the cytoplasm. Nutlin-3 treatment induced a concentration dependent decrease in the hDM2–RFP MCRAID-Ch3 signal that was consistent with the redistribution of the hDM2–RFP from the nucleus to the cytoplasm. Nutlin-3 consistently exhibited an IC_{50} of 0.608 ± 0.382 μM ($n = 5$) for the disruption of the p53–hDM2 PPIs

9. Trypsin 0.25 %, 1 g/L EDTA solution.
10. Recombinant adenovirus p53–GFP and hDM2–RFP Biosensors: Recombinant adenovirus expression constructs bearing the individual p53–GFP (TagGFP, Evrogen, Inc.) and hDM2–RFP (Tag RFP, Evrogen, Inc.) protein-protein interaction partners were obtained from Cyprotex [1, 2].
11. 384-well collagen-coated barcoded assay microplate.

3 Methods

1. Aspirate spent tissue culture medium from U-2 OS cells in tissue culture flasks that are <70 % confluent (*see* **Note 1**), wash cell monolayers 1× with PBS, and expose cells to trypsin-EDTA until they detach from the surface of the tissue culture flasks. Add serum containing tissue culture medium to neutralize the trypsin. Transfer the cell suspension to a 50 mL capped sterile centrifuge tube and centrifuge at 500 × *g* for 5 min to pellet the cells. Resuspend cells in serum containing tissue culture medium and count the number of trypan blue excluding viable cells using a hemocytometer.
2. Co-infect 1×10^7 U-2 OS cells with p53–GFP and hDM2–RFP adenovirus by incubating cells with the manufacturer's recommended volume of virus (*see* **Note 2**), typically 5 μL/10^7 cells, in 1.5 mL of culture medium for 1 h at 37 °C, 5 % CO_2 in a humidified incubator with periodic inversion (every 10 min) to maintain cells in suspension.
3. Dilute co-infected cells to 5.6×10^4 cells/mL and dispense 45 μL (2,500 cells) in each well of a 384-well collagen-coated barcoded assay microplate using a liquid handler (*see* **Note 3**).
4. Incubate assay plates overnight at 37 °C, 5 % CO_2 in a humidified incubator (*see* **Note 4**).
5. Use an automated liquid handling device to add diluted compounds or plate controls (Nutlin3, 10 μM final, or 5 μL of DMSO, 0.25–0.5 % final) to appropriate wells for a final screening concentration of 25 μM (*see* **Note 5**).
6. Incubate plates at 37 °C, 5 % CO_2 in a humidified incubator for 90 min (*see* **Note 6**).
7. Fix samples by the adding 50 μL of pre-warmed (37 °C) 7.4 % formaldehyde and 2 μg/mL Hoechst 33342 in PBS using a liquid handler and incubate at room temperature for 30 min (*see* **Note 7**).
8. Aspirate the liquid and wash the plates twice with 85 μL of PBS using a liquid handler (*see* **Note 8**). Seal with adhesive aluminum plate seals (Abgene) with the last 85 μL wash of PBS in place.

9. Acquire fluorescent images in three channels on an automated imaging platform (*see* **Note 9**) (e.g. ArrayScan VTI, Thermofisher Scientific) (Fig. 2). Images of three fluorescent channels (Hoechst, GFP, and RFP) are sequentially acquired on an ArrayScan VTI platform using either a 10× 0.3 NA or a 20× 0.4 NA objective with the XF93 excitation and emission filter set (Hoechst, FITC, and TRITC) (Fig. 2). In our system, excitation is provided by an X-CITE™ 120 W high pressure metal halide arc lamp with Intelli-Lamp™ technology (Photonic Solutions Inc. Mississauga, Canada), and images are captured on a high sensitivity cooled Orca CCD Camera (Photometrics Quantix). Typically with the 10× 0.3 NA objective, the ArrayScan VTI platform is set up to acquire 250 selected objects (nuclei) or two fields of view, whichever comes first. With the 20× 0.4 NA objective, the ArrayScan VTI platform is set up to acquire four fields of view.
10. Analyze the images of the three fluorescent channels (Hoechst, GFP, and RFP) of the p53–hDM2 PPIB using the molecular translocation image analysis algorithm as described above (Fig. 3) (*see* **Note 10**). The MCRAID-Ch3 output is utilized to quantify the disruption of p53–hDM2 PPIs (Fig. 3b).

4 Notes

1. Typically better responses are obtained when the p53–hDM2 adenovirus biosensors are used to co-infect U-2 OS cells harvested from tissue culture flasks that are <70 % confluent.
2. The optimal volume of each batch of recombinant adenovirus biosensor per 10^6 U-2 OS cells is determined empirically in virus titration experiments. Increasing amounts of virus are incubated with the same number of cells and then the levels of biosensor expression and % of cells infected are determined on the HCS platform after 24 h in culture. Performing infections in cells suspended in a low volume of media combined with periodic inversion (every 10 min) to maintain cells in suspension enhances both the rate of infection and expression levels.
3. Determining the optimal cell seeding density is a critical assay development parameter for any cell-based assay, and especially for HCS assays. The objective is to minimize the cell culture burden while ensuring that sufficient cells are captured per image to give statistical significance to the image analysis parameters of interest. Typically variability increases as the number of cells captured and analyzed decreases.

4. The optimal length of time in culture post viral infection should be determined empirically for each adenovirus biosensor. In general, we have found 24 h post infection to be optimal for most recombinant adenovirus biosensor constructs.
5. Determining the DMSO tolerance is a critical assay development parameter for any cell-based assay, and especially for HCS assays. DMSO has two major effects on HCS assays [1–3, 8, 9, 12, 13]. At DMSO concentrations $\geq$5 % there is a significant cell loss due to cytotoxicity and/or reduced cell adherence. At DMSO concentrations >1 % but <5 %, cells change from a well-spread and well-attached morphology to a more rounded loosely attached morphology that interferes with the ability of the image analysis algorithm to segment images into distinct cytoplasm and nuclear regions. The maximum DMSO tolerance of the HCS assay and the stock concentration of the compound library are the major determining factors of the compound concentration selected for primary screening, confirmation, and follow-up studies.
6. Determining the appropriate compound exposure period is a critical assay development parameter for any cell-based assay, including HCS assays, and should be determined empirically for each new assay. Longer compound exposure periods can result in increased levels of cytotoxicity, which may significantly hinder the ability to make reliable measurements.
7. Determining appropriate cell fixation and nuclear staining conditions is a critical assay development parameter for all end point HCS assays. Combining cell fixation with Hoechst nuclear staining in a single procedure saves time and reduces the number of steps in the protocol. Cell fixation is also important because the scanning and acquisition of a full 96-well or 384-well assay plate on an automated imaging platform depends upon the number of fluorescent channels and images captured per well and the focusing options selected. Scanning times may range anywhere from 10–15 min to 2–3 h per plate depending upon the complexity of the image acquisition procedure.
8. To control and reduce environmental exposure levels to formaldehyde and for long term storage of fixed assay plates, we recommend the aspiration and washing of plates on an automated plate washing platform.
9. Although we have described the image acquisition process on the ArrayScan VTI platform, most automated imaging platforms designed for HCS would be capable of capturing these images.
10. Although we have described the image analysis of the molecular translocation algorithm provided by the ArrayScan VTI platform, most automated imaging platforms designed for HCS provide similar image analysis programs that would be capable of analyzing these images.

References

1. Dudgeon D, Shinde SN, Shun TY, Lazo JS, Strock CJ, Giuliano KA, Taylor DL, Johnston PA, Johnston PA (2010) Characterization and optimization of a novel protein-protein interaction biosensor HCS assay to identify disruptors of the interactions between p53 and hDM2. Assay Drug Dev Technol 8:437–458
2. Dudgeon D, Shinde SN, Hua Y, Shun TY, Lazo JS, Strock CJ, Giuliano KA, Taylor DL, Johnston PA, Johnston PA (2010) Implementation of a 220,000 compound HCS campaign to identify disruptors of the interaction between p53 and hDM2, and characterization of the confirmed hits. J Biomol Screen 15:152–174
3. Johnston PA, Shinde SN, Hua Y, Shun TY, Lazo JS, Day BW (2012) Development and validation of a high-content screening assay to identify inhibitors of cytoplasmic dynein-mediated transport of glucocorticoid receptor to the nucleus. Assay Drug Dev Technol 10:432–456
4. Knauer S, Moodt S, Berg T, Liebel U, Pepperkok R, Stauber RH (2005) Translocation biosensors to study signal-specific nucleocytoplasmic transport, protease activity and protein-protein interactions. Traffic 6:594–606
5. Knauer S, Stauber RH (2005) Development of an autofluorescent translocation biosensor system to investigate protein-protein interactions in living cells. Anal Chem 77:4815–4820
6. Lundholt B, Heydorn A, Bjorn SP, Praestegaard M (2006) A simple cell-based HTS assay system to screen for inhibitors of p53-Hdm2 protein-protein interactions. Assay Drug Dev Technol 4:679–688
7. Stauber R, Afonina E, Gulnik S, Erickson J, Pavlakis GN (1998) Analysis of intracellular trafficking and interactions of cytoplasmic HIV-1 rev mutants in living cells. Virology 251:38–48
8. Trask O, Nickischer D, Burton A, Williams RG, Kandasamy RA, Johnston PA, Johnston PA (2009) High-throughput automated confocal microscopy imaging screen of a kinase-focused library to identify p38 mitogen-activated protein kinase inhibitors using the GE InCell 3000 analyzer. Methods Mol Biol 565:159–186
9. Trask OJ Jr, Baker A, Williams RG et al (2006) Assay development and case history of a 32 K-biased library high-content MK2-EGFP translocation screen to identify p38 mitogen-activated protein kinase inhibitors on the ArrayScan 3.1 imaging platform. Methods Enzymol 414:419–439
10. Kumar S, Saradhi M, Chaturvedi NK, Tyagi RK (2006) Intracellular localization and nucleocytoplasmic trafficking of steroid receptors: an overview. Mol Cell Endocrinol 246:147–156
11. Stauber R (2002) Analysis of nucleocytoplasmic transport using green fluorescent protein. Methods Mol Biol 183:181–198
12. Nickischer D, Laethem C, Trask OJ Jr et al (2006) Development and implementation of three mitogen-activated protein kinase (MAPK) signaling pathway imaging assays to provide MAPK module selectivity profiling for kinase inhibitors: MK2-EGFP translocation, c-Jun, and ERK activation. Methods Enzymol 414:389–418
13. Williams RG, Kandasamy R, Nickischer D et al (2006) Generation and characterization of a stable MK2-EGFP cell line and subsequent development of a high-content imaging assay on the Cellomics ArrayScan platform to screen for p38 mitogen-activated protein kinase inhibitors. Methods Enzymol 414:364–389